Available online at www.sciencedirect.com
ScienceDirect
International Journal of Thermal Sciences 47 (2008) 778–786
International Journal of Thermal Sciences
www.elsevier.com/locate/ijts

Shape optimization of a MHD generator based on pressure drop and power output constraints

S.M. Aithal *

HyPerComp Inc., 31255 Cedar Valley Dr, Suite # 327, Westlake Village, CA 91362, USA

Received 20 March 2007; received in revised form 4 June 2007; accepted 5 June 2007

Available online 5 July 2007

Abstract

The optimum shape and axial variation of electrical loading (power ratio) of a MHD generator are obtained for a prescribed fractional power output and pressure drop along the generator. These optimum solutions are obtained using the ADS (Automatic Design Synthesis) optimization code. The objective function (duct size) for the prescribed design conditions was obtained by Carter for a quasi 1-D flow with a simple power law model for electrical conductivity. In this work, a generalized numerical optimization scheme, capable of incorporating any arbitrary electrical conductivity model is presented. The numerical solutions obtained using this scheme is validated with analytical results obtained by Carter. We demonstrate the use of this scheme to minimize the volume of a duct with a hypothetical power law model incorporating the effect of residence time (function of inlet Mach number) on the electrical conductivity. We further demonstrate the use of this scheme for obtaining the optimum shape of a MHD generator using an E-beam generated ionized gas stream.

Keywords: Optimization; MHD generator; Variable electrical conductivity; Power ratio

1. Introduction

A MHD generator essentially converts the kinetic energy of a conducting fluid directly into electrical energy without the use of any rotating machinery. MHD-based power generation has several economic and ecological advantages. Higher efficiencies, lack of rotating machinery (turbines), reduced maintenance costs, less warm water effluents are some of the advantages of using MHD-based power generation. Due to these reasons, there was a flurry of activity in developing ground-based MHD generators in the sixties and early seventies. Open-cycle and closed-cycle MHD generators were the two main kinds of MHD systems under consideration, classified on the basis of the working fluid and the heat source. Open-cycle MHD generators usually operate with the combustion products of fossil fuels as the working fluid. Closed-cycle MHD generators, usually more suitable for operating with nuclear reactor heat sources, use a seeded noble gas or liquid metal as the working fluid. In this paper, our focus is on a MHD generator with an ionized gas (plasma) stream as the working fluid.

Due to economic reasons and technical hurdles, research and development in ground-based MHD power generation slowed in the eighties and early nineties. In the recent years, there has been a resurgence of interest in MHD systems for aerospace applications. The possibility of using a MHD power generator at the inlet of an air-breathing hypersonic engine has received considerable attention since the mid-nineties ([1–4] and references therein). The generated electricity could be used to power various devices on-board or to provide MHD acceleration of the engine exhaust flow (MHD-bypass concept). Additionally, the MHD generator could be used as a means to reduce total enthalpy at the engine inlet and could thus be used as a control device to allow operation of scramjets under off-design conditions. Given the potential impact of MHD generators in aerospace applications, there is a great need for design, analysis and optimization of MHD generators.

Design and analysis of MHD-based systems is a difficult task. Multi-dimensional simulation of the fluid-flow and heat transfer characteristics of an MHD generator is beset with

* Tel.: +1 818 865 3710 (112); fax: +1 818 865 3711.
E-mail address: shashi@hypercomp.net.

1290-0729/$ – see front matter
doi:10.1016/j.ijthermalsci.2007.06.002

Nomenclature

B	magnetic field
C_p	specific heat per mass unit at constant pressure
E	electric field
J	current density
K	power ratio (electrical loading factor)
M	Mach number
p	pressure
P_{so}	stagnation pressure at the duct inlet
R	gas constant (per unit mass)
T	temperature
T_{so}	stagnation temperature at the duct inlet
u	velocity
W	mass flow rate
x	distance along the channel

Greek symbols

β	constant
δ	variable used in the definition of ratio between stagnation pressure at the inlet to the stagnation pressure at any given location in the channel
ν	natural logarithm of ratio between stagnation temperature at the inlet to the stagnation temperature at any given location in the channel
σ	electrical conductivity
γ	ratio of specific heats
ρ	density

several challenges. The governing equations are coupled nonlinear PDEs with additional complexity due to the Lorentz forces in the momentum equation and an associated Joulean heating term in the energy equation. An accurate calculation of these terms requires the flow equations to be coupled with an equation describing the electric potential, thus making it difficult for numerical simulations. Additionally, the computational effort is another important consideration in the use of multidimensional simulations of MHD generators.

Design of practical MHD-based systems depends on several constraints such as overall system efficiency, cost and size. Simplified analyses based on quasi 1-D assumptions can be of great value in the design/analysis of MHD-based system. Before tackling the overall system issues, it is necessary to examine the feasibility of operating MHD channels and optimizing them for a given set of objective function and design constraints. The MHD generator could be optimized for one of many quantities, based on system design considerations. For example, one could minimize the duct size to reduce heat losses and reduce material cost, or one could optimize the maximum power density for a given size of the MHD generator. The overall system design can be greatly facilitated if the designer could optimize the generator for different criteria and constraints and pick the configuration best suited for a practical engine design.

The electrical conductivity is an important aspect in the design and operation of a MHD-generator, particularly for aerospace applications. While seeding was considered as a prime candidate for enhancing the electrical conductivity of ground-based MHD generators, several non-equilibrium techniques have been suggested for aerospace applications [4]. In order to study the design and optimization of MHD generators, it is necessary to incorporate a realistic electrical conductivity model in the analysis. Hence there is a need to develop a framework to conduct optimization studies wherein; any arbitrary electrical conductivity model can be used by the designer. Several design, analysis and optimization studies exist with regards to ground-based MHD generators [5–16]. Optimization studies such as [5–7] were conducted with several simplifying assumptions and analytical expressions for an objective function was derived for a given set of design conditions/constraints. These analyses assumed the electrical conductivity to be constant or obey some prescribed power law dependence. Neuringer [5] considered the problem of optimizing power from a channel with a constant cross-section and uniform electrical conductivity. Swift-Hook and Wright [6] considered the problem of minimizing the duct length/volume for a constant Mach-number generator. They assumed an electrical conductivity model having a power law dependence on temperature and pressure. Carter [7] extended the analysis of [6] to optimize the size of a MHD generator for a given power output and a given pressure drop. If the electrical conductivity were assumed to be dependent only on pressure and temperature, Carter's analysis could optimize both the gas velocity (Mach number) and electrical loading factor (power ratio) along the length of the duct. Carter further extended the electrical conductivity model of Swift-Hook and Wright to include the effects of elevated electron temperatures. A power law dependence on $(uB - E)/p$ was used to incorporate the effects of velocity and K (local power ratio). With this electrical conductivity model, however, Carter's analysis was unable to optimize inlet gas velocity (Mach number). The MHD duct could be optimized for minimum size for a prescribed inlet Mach number, yielding the optimum axial variation of the power ratio (K).

In this work, we have extended Carter's analysis to include any arbitrary conductivity model. The optimization is accomplished using a general-purpose optimization program called ADS [17]. The numerical scheme developed in this paper can be used to optimize the size of a MHD generator for any given electrical conductivity model or discrete axial electrical conductivity distribution for a prescribed power output and pressure drop. We have validated this numerical scheme by comparing our results with the analytical results of Ref. [7]. We have further demonstrated the generality of our scheme by introducing a hypothetical conductivity model that not only captures the effects of elevated electron temperatures due to the electric field, but also accounts for the effect of residence time on the electrical conductivity. With this simple electrical conductivity model, we have shown that it is possible to optimize the

size of the MHD duct while optimizing both the inlet Mach number and the axial variation of the electrical loading. Using our optimization scheme, we further demonstrate its use in optimizing a MHD generator, using non-equilibrium ionization techniques for possible hypersonic aerospace applications. We have done so to demonstrate ability of our numerical framework to compute realistic variable electrical conductivity using finite-rate chemical kinetic models. E-beams are considered to be the most energy-efficient non-equilibrium ionization technique [4,18]. Hence, as an example, we investigate the optimization of a MHD generator with e-beam generated air plasma. An experimentally validated e-beam chemistry model [19] is used to compute the electrical conductivity in our optimization framework. We present optimization of the MHD-generator volume for various e-beam electron production rates and free-stream pressures.

2. Basic equations and theory

In this paper, we follow the analysis of Carter [7] for optimizing an infinitely segmented Faraday generator. The calculations use a 1-D flow model of a perfect gas with constant specific heat. The electrical conductivity and Mach number are allowed to vary along the length of the channel. The magnetic field is assumed to be constant and the axial currents are assumed to be zero.

The quasi 1-D steady flow equations are as follows:

$$\text{Continuity equation:} \quad \rho u A = W \tag{1}$$

$$\text{Momentum equation:} \quad \rho u \frac{\mathrm{d}u}{\mathrm{d}x} + \frac{\mathrm{d}p}{\mathrm{d}x} + JB = 0 \tag{2}$$

$$\text{Energy equation:} \quad \rho u \frac{\mathrm{d}}{\mathrm{d}x}\left(C_p T + \frac{1}{2}u^2\right) + JE = 0 \tag{3}$$

$$\text{Equation of state:} \quad P = \rho R T \tag{4}$$

$$\text{Modified Ohm's law:} \quad J = \sigma u B(1 - K) \tag{5}$$

In the above equation, the electrical load factor K is defined as the fraction of the total power generated that is actually extracted. In an MHD generator, the total MHD power generated per unit volume is JBu. From the total power generated, the total power extracted is JE, while the remainder (J^2/σ) is dissipated as Ohmic loss in the gas. Based on these considerations, the electrical loading factor, $K = E/uB$. For a MHD generator, $0 < K < 1$.

In Ref. [7], the electrical conductivity of the gas is given by the power law

$$\sigma = Q\left(\frac{T}{T_{so}}\right)^{y}\left(\frac{P}{P_{so}}\right)^{-(z+w)}(X)^{w/2}(1-K)^{w} \tag{6}$$

where Q, y, z, w, T_{so} and P_{so} are given constants and

$$X = \frac{u^2}{2C_p T} = \frac{(\gamma-1)}{2}M^2$$

where

$$C_p = \frac{\gamma}{(\gamma-1)}R; \qquad M = \frac{u}{\sqrt{\gamma R T}}$$

The electrical conductivity model in Eq. (6) was an improvement of the power-law model suggested in Ref. [6]. The power-law model suggested in Ref. [6] is a phenomenological model, relating the electrical conductivity to temperature and pressure of the gas. Carter extended it to include the effect of elevated electron temperature by introducing a power-law dependence on $(uB - E)/p$. Thermal ionization of a gas, leading to the production of charged species and hence higher conductivity, is directly proportional to the gas temperature. The collision frequency of the charged species with neutrals acts as a opposing force or "drag" on the charged species against the influence of the electric field. At higher pressures, the collision frequency between charged species and neutrals increase leading to a reduction in the conductivity. Also, at higher pressures the possibility of recombination of positive and negative species via collisions is higher. Hence the electrical conductivity scales inversely as the pressure. The influence of electric field is to accelerate the electrons to energies appreciably higher than the thermal energy. At lower pressures, the mean-free-path of electrons is higher allowing the electrons to acquire greater energy. These ideas form the basis for the expression for electrical conductivity given in Eq. (6). The weakness of the conductivity model suggested by Carter is that it does not take into consideration the effect of gas velocity (proportional to X) on "residence time" and its impact on the gas kinetics for producing charged species. Hence, the model would lead to a monotonic decrease in duct-size with increasing gas velocity. This issue has been addressed in Section 4.2 where the conductivity model is modified to include the effect of residence time on the gas kinetics. In the examples discussed by Carter, the typical values of 'y' range from 7 to 11, typical values of 'z' range from 0.6 to 1 and the typical values of 'w' range from 0 to 4. The value of 'w' $= 0$ implies that the electrical conductivity is not influenced by the electric field (no elevated electron temperature effects).

The flow equations can be expressed in terms of the stagnation values using the adiabatic law

$$\ln\left(\frac{p_s}{p}\right) = \beta \ln\left(\frac{T_s}{T}\right) = \beta \ln(1+X) \tag{7}$$

where, $\beta = \frac{\gamma}{\gamma-1}$.

Eq. (7) can be written as

$$\frac{1}{p}\frac{\mathrm{d}p}{\mathrm{d}x} = \frac{1}{p_s}\frac{\mathrm{d}p_s}{\mathrm{d}x} - \frac{\beta}{1+X}\frac{\mathrm{d}}{\mathrm{d}x}(1+X)$$

Eqs. (2) and (3) can be written as

$$\frac{1}{p_s}\frac{\mathrm{d}p_s}{\mathrm{d}x} + \frac{\beta X}{T_s}\frac{\mathrm{d}T_s}{\mathrm{d}x} + \frac{\sigma u B^2(1-K)}{p} = 0 \tag{8}$$

$$\frac{\beta(1+X)}{KT_s}\frac{\mathrm{d}T_s}{\mathrm{d}x} + \frac{\sigma u B^2(1-K)}{p} = 0 \tag{9}$$

Assume,

$$\ln\left(\frac{p_{so}}{p_s}\right) = \beta(\delta+\nu); \qquad \ln\left(\frac{T_{so}}{T_s}\right) = \nu \tag{10}$$

In Eq. (10) P_{so} and T_{so} are the stagnation pressure and temperature at the inlet of the duct. P_s and T_s are the stagnation conditions at any point in the duct. At the inlet, $P_s = P_{so}$ and

$T_{so} = T_s$, hence $\delta = \nu = 0$. The fractional power output, and hence the value of ν at the exit is decided by the designer. The pressure ratio is a design parameter usually fixed by the compressor power; hence the value of $\beta(\delta + \nu)$ at the exit is fixed. Hence at the exit, we have, $\nu = \nu_1$ (prescribed on the basis of the fractional power output) and $\delta = \delta_1$. For a given value of fractional power output (based on ν_1) and pressure ratio, δ would be a function of ν. Based on Eqs. (7) and (10), X would also be a function of ν.

Eqs. (8) and (9) can be used to get

$$\frac{\mathrm{d}\delta}{\mathrm{d}\nu} = \frac{(1+X)(1-K)}{K} \tag{11}$$

$$\frac{\mathrm{d}x}{\mathrm{d}\nu} = \frac{\beta(1+X)p}{\sigma B^2(2\beta RTX)^{1/2}K(1-K)} \tag{12}$$

The optimization problem is to determine the variation of $X(\nu)$ and $K(\nu)$ for a given value of ν_1 and $\beta(\delta_1 + \nu_1)$, so as to minimize the duct size. For a constant Mach number generator, the fractional output power is $(1 - \mathrm{e}^{-\nu})$ [6]. The designer could be interested in either reducing the length, the cross-sectional area or the volume of the duct for a given set of fractional output power and pressure ratio $(= \mathrm{e}^{-\beta(\delta 1+\nu 1)})$. The general form of the duct size can be written as,

$$S(n) = \int_0^{\nu_1} A(x)^n \frac{\mathrm{d}x}{\mathrm{d}\nu}\,\mathrm{d}\nu \tag{13}$$

where, $A(x)$ is the cross-sectional area of the duct and $\delta = \delta_1$ at $\nu = \nu_1$ at the end of the duct.

Based on Eq. (13), the designer might choose to minimize duct length ($n = 0$), duct surface area ($n = 1/2$) or duct volume ($n = 1$). Heat losses and friction have a large impact on the performance of the MHD generator. Cost of the magnetic field is also an important design consideration. Heat losses and the magnetic field are proportional to the surface area. Hence, if the designer wants to optimize the shape of the MHD generator for a given power output and pressure ratio, it is best to minimize the surface area from an overall design standpoint. As mentioned above, this could be accomplished by choosing $n = 1/2$ in Eq. (13) (for a duct with a square cross-section the minimum duct surface area would be $4S(1/2)$). In general, minimization of Eq. (13) would yield the optimum variation of $X(\nu)$ and $K(\nu)$ for a given value of ν_1 for a chosen value of n.

At this point, our analysis deviates from that outlined by Carter. Carter simplified Eq. (12) using the power law for electrical conductivity (Eq. (6)). The simplified expression for $\frac{\mathrm{d}x}{\mathrm{d}\nu}$ is used in Eq. (13). Carter minimized the simplified form of Eq. (13) to obtain analytical expressions for the variation of X and K as functions of the power law exponents, namely w, y and z. These analytical expressions are valid only if the electrical conductivity (σ) can be expressed in the power law form shown in Eq. (6), and hence are of limited usefulness in optimizing MHD generators where the electrical conductivity may not obey such a power law, as in the case with non-equilibrium ionization methods.

In this work, Eq. (13) is the cost (objective) function that is minimized using the ADS optimization code, without making any simplification for the electrical conductivity in Eq. (12). Any given model of electrical conductivity can be incorporated in this numerical scheme to optimize the duct size. The numerical scheme is explained in the next section.

3. Numerical scheme

The cost function to be minimized is Eq. (13) subject to the following conditions

1. X and δ are functions of ν;
2. $\delta = \delta_1$ at $\nu = \nu_1$ at the end of the duct;
3. $\delta = \nu = 0$ at the entrance of the duct;
4. K is determined by an algebraic simplification of Eq. (11), namely

$$K = \left[1 + \frac{1}{(1+X)}\frac{\mathrm{d}\delta}{\mathrm{d}\nu}\right]^{-1} \tag{14}$$

The reasons for conditions 1–3 were explained in Section 2. Conditions 1, 2 and 3 can be satisfied if one assumes the following expression for δ.

$$\delta(\nu) = A\big(1 - \exp(-B\nu)\big) \tag{15}$$

where,

$$B = -\frac{1}{\nu_1}\ln\left(1 - \frac{\delta_1}{A}\right)$$

Similarly, $X(\nu)$ can be written as

$$X(\nu) = X_1 + X_2\big(1 - \exp(-X_3\nu)\big) \tag{16}$$

A, X_1, X_2, X_3 are the four design variables that can be varied to minimize the cost function for a given δ_1 and ν_1. In this work, we present results for cases wherein there are only two design variables, namely, A and X_1. In other words, K is a function of ν, whereas X (and hence Mach number) is constant along the length of the generator. We assume a constant Mach number for the optimization process since Carter shows that the reduction in the optimum duct size with a varying Mach number is less than a fraction of a percent as compared to a constant Mach number duct.

The ADS solver is used to minimize Eq. (13) using a gradient-based optimization technique explained below. The ADS code solves the non-linear constrained optimization problem

Minimize $f(\vec{X})$

subject to the inequality constraints

$$G_j(\vec{X}) \leqslant 0, \quad j = 1, N_j$$

and equality constraints

$$H_k(\vec{X}) = 0, \quad k = 1, N_k$$

where the vector $\vec{X} = (x_1, x_2, x_3, \ldots, x_N)$ is the vector of design parameters. ADS employs the method of steepest descent which leads to the iterative solution procedure for $\vec{X}$ given by

$$\vec{X}^{n+1} = \vec{X}^n + c.\vec{S}^n$$

where the superscript n is the iteration counter (optimization cycle), $\vec{S}$ is the vector search direction, and c is a scaling parameter. The optimization routine converges when the relative and absolute change in the objective function are less than a user-defined convergence criterion. If $F(0)$ were to be the value of the objective function corresponding to the initial design, the absolute change in the objective function is defined as $\varepsilon F(0)$. In this work, ε was set equal to 0.001. The relative change in the objective function is defined as $\|(f(\vec{X}^{n+1}) - f(\vec{X}^n))/(f(\vec{X}^n))\|$. The convergence criterion for relative change in the objective function was set equal to 0.001.

Initial values are chosen for the design variables A and X_1. As explained above, any conductivity model can be used to evaluate Eq. (12) (which is a part of the integrand in Eq. (13)). In Section 4.3 we show how a finite-rate chemistry model can be used to obtain a spatially varying electrical conductivity, which is then used to evaluate Eq. (12). Eq. (13) is integrated numerically using an integration step of $10^{-4}\nu$ to obtain the cost function. The ADS optimizer uses this cost function to vary the design variables (A and X_1), using the procedure explained above to obtain the optimum cost function. The design variables (A and X_1) corresponding to the optimum value are then used to evaluate $K(\nu)$ and $X(\nu)$, using Eqs. (14)–(16).

4. Results and discussions

In this section, we demonstrate the use of our numerical scheme to minimize the volume of a MHD generator for a given fractional power output and pressure ratio. We do so, using conductivity models with increasing degrees of complexity as outlined below

- Power law conductivity model: We validate our numerical scheme comparing our results with the analytical solutions for the power law conductivity model proposed by Carter (Eq. (6)).
- Extended power law conductivity model: We extend Carter's power law conductivity model to account for the effect of residence time of the gas flow on the electrical conductivity. This new conductivity model yields the optimum inlet Mach number and the optimum variation of the electric loading factor along the duct, for minimum duct size.
- Finite-rate e-beam induced air chemistry plasma model: An experimentally validated finite-rate chemistry model is used to demonstrate the use of the proposed scheme to compute realistic electrical conductivities based on finite-rate chemical kinetics. Optimum inlet Mach number and variation of electrical loading factor along the duct is obtained using this electrical conductivity model.

4.1. Validation: Power law conductivity model

We validate our numerical scheme by comparing our results with those presented by Carter. Carter discusses the results of minimizing the volume of a MHD duct for a set of conditions and power-law exponents given in Table 1.

Table 1
Optimization conditions for minimization of duct volume in Ref. [7]

Variable	Value
γ	1.667
ν_1	0.4005
u_1	0.25
τ ($\tau = \nu_1 + u_1$)	0.65
w	4.0
y	7.0
z	0.6
$X(\nu)$	2.0
M	$\sqrt{6}$

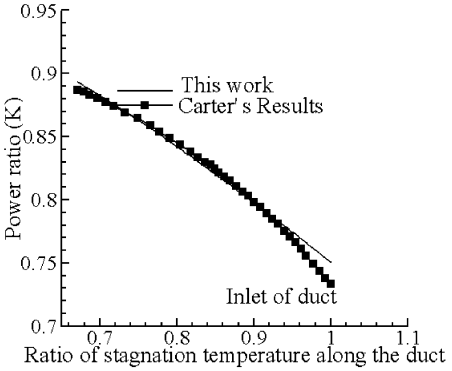

Fig. 1. Comparison of power ratio as a function of ratio of stagnation temperature.

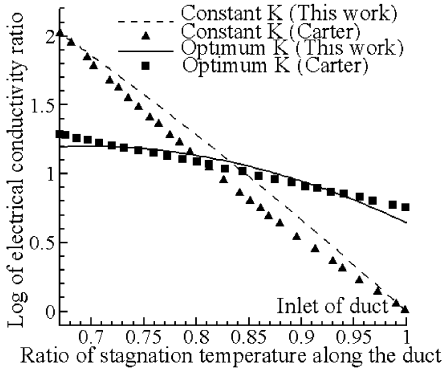

Fig. 2. Comparison of electrical conductivity for cases (a) and (b).

Carter points out that his conductivity model [Eq. (6)], accounting for the effect of elevated electron temperatures on electrical conductivity, is unable to optimize inlet Mach numbers. Hence the inlet Mach number is prescribed and held fixed along the MHD generator. The optimum variation of electrical loading factor (K) along the duct is obtained for a prescribed inlet Mach number ($M = \sqrt{6}$, $X = 2.0$). For these conditions, Carter considers two cases, namely, (a) optimization with K constant along the channel (b) optimization with K varying along the channel. We compare the results of our simulations, obtained using our numerical scheme, with those presented by Carter. Fig. 1 shows a comparison of the variation of the loading factor K as a function of $T_s/T_{so}(e^{-\nu})$.

Fig. 2 shows a comparison of the variation of electrical conductivity as a function T_s/T_{so} for cases (a) and (b).

Table 2
Comparison of numerical results with Ref. [7]

Case	This work	Ref. [7]
Case (a) Constant K	$K = 0.828$	$K = 0.828$
Case (b) Variable K	K varies from 0.7505 to 0.8936	K varies from 0.734 to 0.8889
Reduction in duct volume with variable K	44.8%	44.75%

Evaluating Eq. (19) and Eq. (32) in Ref. [7], it is possible to compare the optimum duct volume for Case (a) and Case (b). Carter's work and our results both show that when K varies axially, the optimum duct volume is only 44.75% of the optimum duct volume for a constant power ratio case. Results from Ref. [7] for these two cases are summarized in Table 2, along with results obtained from our work.

It is seen that the results obtained using the ADS optimization scheme match analytical results well.

4.2. Modified conductivity model

As pointed out earlier, Carter's model for electrical conductivity is unable to predict an optimum inlet Mach number. This conductivity model predicts a continuous decrease in duct size as the inlet Mach number increases. This is because the model requires the conductivity to increase monotonically with increasing Mach number. This model does not take into consideration the reduction in conductivity due to a decrease in the gas residence time at higher Mach numbers. We use our numerical scheme to introduce an electrical conductivity model that rectifies this deficiency in the model prescribed by Carter.

For MHD generators, ionization can be created using seeding and/or other non-equilibrium processes such as e-beams, AC and DC discharges, photo-ionization etc. The air chemistry induced by these non-equilibrium techniques create the charged particles necessary for maintaining the electrical conductivity. Chemistry reaction times scales can be comparable to flow time-scales at low pressures and high Mach numbers. The effect of residence time on electrical conductivity (Eq. 6) can be modeled by a power-law expression of the form shown below.

$$\sigma_m = Q\left(\frac{T}{T_{so}}\right)^{y}\left(\frac{P}{P_{so}}\right)^{-(z+w)}(X)^{w/2}(1-K)^{w}\mathrm{e}^{-\tau X} = \sigma_c e^{-\tau X}$$

where, σ_c is the electrical conductivity from Carter's model.

τX can be viewed as being proportional to the ratio between the chemistry and flow time-scales (flow time-scales inversely proportional to Mach number). Reaction rate constants and the number densities (proportional to pressure) of the reacting species determine the chemistry time-scales (proportional to τ). For a given set of operating conditions, the chemistry time-scales are fairly constant. The flow time-scale of the gas in the MHD generator, on the other hand, depends on the Mach number. A condition where $\tau X = 0$, implies that the chemistry time-scales are much smaller than the flow time-scales and hence the ionization chemistry is not affected by a change in flow time-scales (Mach number). This condition represents the conductivity model proposed by Carter. A condition such as $0 < \tau X < 1$, implies that the flow time-scales are comparable to the chemistry time-scales and hence will have an effect on the electrical conductivity. If $\tau X > 1$, the flow time scales are smaller than the chemistry time scales, and hence the electrical conductivity can be strongly impacted by it. This model captures the behavior of electrical conductivity, wherein the increase in conductivity due to the power law dependence on Mach number ($X^{w/2}$) is countered by a reduction in conductivity due to the decrease in residence time $\mathrm{e}^{-\tau X}$. We present results describing the effect of τ, for two values of prescribed inlet Mach numbers, namely, $M^2 = 6$ and $M^2 = 8$.

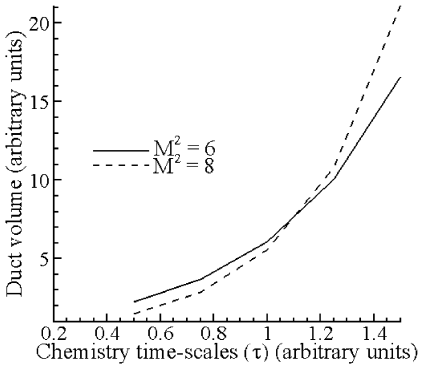

Fig. 3. Variation of duct volume with τ for two different inlet Mach numbers.

Fig. 3 shows the effect of τ on the duct volume for the two different Mach numbers. It is seen that for a given Mach number, increasing τ, increases the optimum duct volume. This is to be expected, since for a given Mach number (flow-time scale) higher τ, represents longer chemistry time-scales. Longer chemistry time-scales for a given flow time-scale simply implies that the ionization kinetics are not able to proceed to completion, leading to a reduction in the electrical conductivity and hence increase in the duct volume. Fig. 3 also shows the opposing effect of Mach number and residence time on the electrical conductivity and hence duct volume. For the particular case discussed here, for small values of τ ($\tau < 1.25$) higher inlet Mach numbers yield lower duct volume. As discussed earlier, small values of τ, imply a lesser impact of residence time on conductivity, hence the trends are as predicted by Carter's model. However, for $\tau > 1.25$, this trend is reversed. The optimized duct volume increases with Mach number, which signifies that conductivity is more strongly affected by residence time.

4.2.1. Optimization of inlet Mach number and loading factor for minimum duct volume

For a given value of τ, the dependence of conductivity on Mach number incorporates two opposing effects (a) the power law dependence on Mach number tends to increase conductivity with increasing Mach numbers (b) the effect of residence time tends to reduce conductivity with an increase in Mach number. The effect of these two opposing effects makes it possible to seek an optimum value of inlet Mach number for which the duct volume (size) can be minimized.

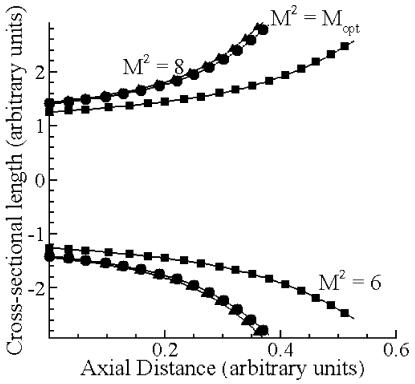

Fig. 4. Optimum duct shape for various inlet Mach numbers.

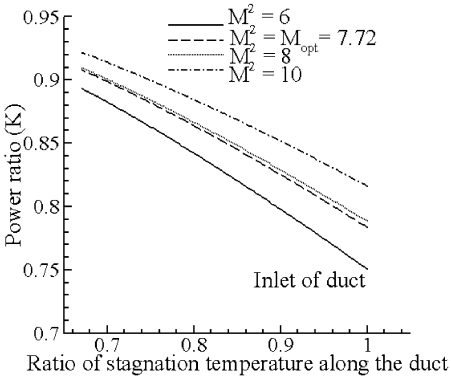

Fig. 5. Variation of power ratio for various inlet Mach numbers.

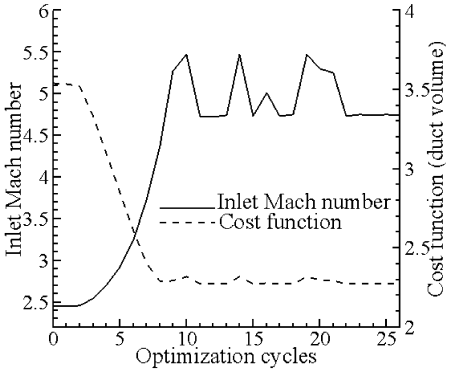

Fig. 6. Cost function and inlet Mach number variation with optimization cycles.

We present results for a case with the same set of power law exponents, ν_1 and τ values outlined in Table 1. We assume $\tau = 1$ in our conductivity model. The optimum value of inlet Mach number for these conditions is $M = 2.78$. Fig. 4 shows the duct shape obtained by plotting the cross-sectional length versus the axial length for $M^2 = 6$, $M^2 = 8$ and $M^2 = M^2_{\text{opt}}$.

Fig. 5 shows the variation of power ratio (K) for different inlet Mach numbers. Variation of K with the optimum inlet Mach number and for fixed inlet Mach numbers of $M^2 = 6$, $M^2 = 8$ and $M^2 = 10$ are shown. It is seen that for a given axial location, the power ratio increases monotonically with inlet Mach number.

Fig. 6 shows the cost function (duct volume) and the design variable (inlet Mach number (left axis)) verses optimization cycle number. From the variation of the cost function and design variable, it is seen that after about 22 optimization cycles, the cost function and Mach number converge to constant values based on the convergence criterion described in Section 3.

Table 3
E-beam chemistry model with reaction rate constants [19]

No.	Reactions	A	n	Ea/R
1	$e^- + 2O_2 = O_2^- + O_2$	2.5E−42 (m^6/s)	0	0
2	$e^- + O_2 + N_2 = O_2^- + N_2$	1.6E−43 (m^6/s)	0	0
3	$e^- + O_2^+ = O_2$	2.0E−12 (m^3/s)	0	0
4	$e^- + N_2^+ = N_2$	2.0E−12 (m^3/s)	0	0
5	$O_2^- + O_2 = 2O_2 + e^-$	2.2E−24 (m^3/s)	0	0
6	$O_2^- + N_2 = O_2 + N_2 + e^-$	1.8e−26 (m^3/s)	0	0
7	$O_2^- + O_2^+ + O_2 = 3O_2$	1.55E−37 (m^6/s)	0	0
8	$O_2^- + O_2^+ + N_2 = 2O_2 + N_2$	1.55E−37 (m^6/s)	0	0
9	$O_2^- + N_2^+ + O_2 = 2O_2 + N_2$	1.55E−37 (m^6/s)	0	0

4.3. Conductivity for e-beam air plasma

The conductivity models used in Sections 4.1 and 4.2 are hypothetical and hence are not of much use in the actual design/optimization studies of MHD generators. The numerical scheme presented in this paper can be used to study spatially varying electrical conductivity based on finite-rate chemical kinetics. As an example, we present results for air plasmas with e-beam induced ionization. We have chosen the e-beam chemistry model to compute the electrical conductivity because the finite-rate chemistry model is experimentally validated [19]. The chemistry model has 9 elementary reactions and 6 species and hence is representative of a fairly complex ionization mechanism to be included in calculation of the electrical conductivity. More detailed air plasma models can also be incorporated in our framework for detailed computations of electrical conductivity. However, for the purpose of demonstrating the effect of electrical conductivity on the shape of the MHD generator, the current model is adequate. The reaction rate constants and reaction mechanism are obtained from Ref. [19] and is given in Table 3.

The model includes processes for electron/ion production by the e-beam (S_o), electron–ion recombination, 3-body ion–ion recombination, electron attachment in 3-body collisions to O_2 and N_2 and electron detachment in collisions with O_2 and N_2. Since the e-beam produces an electron-ion pair, the e-beam generated electrons and ions are added to the source term of species continuity equations for electrons and ions as shown below,

$$\frac{dn_e}{dt} = S_o + \omega_e$$

$$\frac{dn_+}{dt} = S_o + \omega_i$$

where, ω_e and ω_i are the net rates of production of the electrons and positive ions (N_2^+ and O_2^+) respectively. The species considered in this chemistry model are N_2^+, O_2^+, O_2^-, O_2, N_2, $e-$.

For a given beam current and voltage, the electron/ion production of the e-beam (S_o) depends on density [20]. The effect

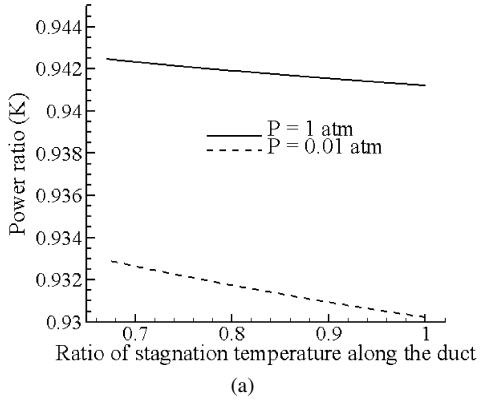

(a)

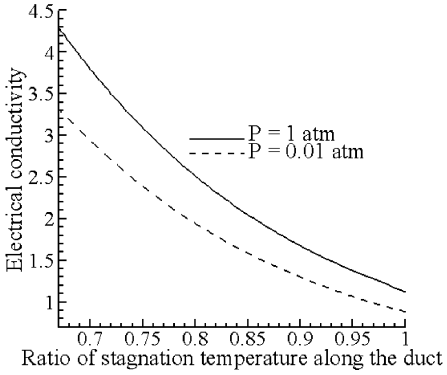

(b)

Fig. 7. Variation of power ratio (a) and electrical conductivity (mho/m) (b) as a function of T_s/T_{so} for two different free-stream pressures.

of free-stream pressure and cross-sectional area on S_o is modeled by using an expression of the form

$$S_o = S_c \frac{p}{p_a A(x)}$$

where, $S_c = 1.5\text{E}24\ \#/\text{m}^3$ [19] evaluated at 1 atmosphere for a beam current of 5 mA/cm^2 and beam voltage of 60 keV, $A(x)$ is the cross-sectional area at a location x in the duct, p is the pressure and p_a is 1 atmosphere.

The variation of pressure and cross-sectional area along the duct gives rise to an axial variation of charged and neutral species. This variation in species number density leads to an axially varying electrical conductivity. In our numerical framework, we solve the coupled finite-rate chemistry equations for the chemistry model given in Table 3 at each axial location (corresponding to a given value of ν). From the solution of these coupled finite rate chemistry equations, the concentration of the charged and neutral species at each location is known. Using the expression for electrical conductivity [21], it is possible to compute the electrical conductivity at a given axial location, which is then used in the computation of the overall cost function.

Based on the e-beam model described above, we studied the problem of minimizing the duct volume for $\nu_1 = 0.4$, $\gamma = 1.667$ and $\tau = 0.65$ (same as values in Table 1) at two different pressures, namely, $P = 1$ atm and $P = 0.01$ atm. The electron–ion recombination rate for reactions 3 and 4 (Table 3) is 2.0×10^{-12} m^3/s^{-1} at 1 atm [19], while it is 2.0×10^{-13} m^3/s^{-1} at 0.01 atm [18]. Fig. 7 (a) and (b) shows the variation in power ratio and electrical conductivity (mho/m) along the duct (shown as a function of T/T_{so}), computed using the e-beam chemistry model.

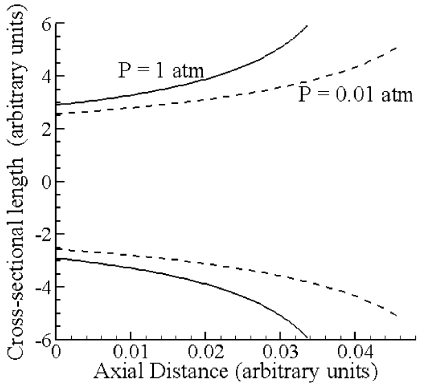

Fig. 8. Optimized shape of the duct at $P = 1$ atm and $P = 0.01$ atm.

It is seen that the reduction in S_o at lower pressure leads to a lower electrical conductivity, in spite of a lower electron-ion recombination rate. Fig. 8 shows the shapes of the MHD ducts at $P = 1$ atm and 0.01 atm obtained by plotting the lengths and cross-sectional areas. It is seen that the freestream pressure impacts the shape of the MHD generator quite significantly.

The computing time required for shape optimization problem with the e-beam induced ionization was about 10 minutes on a single CPU 2.5 GHz machine. Obtaining the species concentrations from a system of ODEs describing the finite-rate chemical kinetics took a major portion of the total computing time.

5. Summary and conclusions

The problem of optimizing the shape of a MHD duct for a given fractional power output and pressure drop has been investigated numerically using the ADS optimization code. The cost function was evaluated using the 1-D flow model as prescribed by Carter. The numerical methodology used in this work enables the use of any arbitrary electrical model for the optimization problem under consideration. We have validated our numerical scheme with the results presented by Carter. Furthermore, we have used this numerical scheme to study the shape optimization problem for MHD ducts with e-beam induced ionization of the air stream. Axially varying electrical conductivities were obtained by a finite-rate chemistry model describing the e-beam induced ionization. The computing time required for the shape optimization problem of a MHD duct coupled with a finite-rate chemistry model describing the non-equilibrium ionization is on the order of minutes. The versatility and the short computing time make this numerical scheme a viable tool for design/optimization studies in MHD generator applications.

References

[1] V.L. Fraishtadt, A.L. Kuranov, E.G. Sheikin, Techn. Phys. 43 (1998) 1309–1313.

[2] E.P. Gurijanov, P.T. Harsha, AJAX: New directions in hypersonic technology, in: AIAA-96-4609, Seventh Aerospace Planes and Hypersonics Technology Conference, Norfolk, VA, 1996.
[3] R.C. Murray, S.H. Zaidi, M.R. Carraro, L.M. Valilyak, S.O. Macheret, M.N. Shneider, R.B. Miles, Observation of MHD effects with non-equilibrium ionization in cold supersonic air flows, in: AIAA-2004-1025, 42nd AIAA Aerospace Sciences Meeting & Exhibit, Reno, NV 2004.
[4] S.O. Macheret, M.N. Shneider, R.B. Miles, Potential performance of supersonic MHD power generators, in: AIAA-2001-0795, AIAA 39th Aerospace Sciences Meeting & Exhibit, 8–11 January 2001, Reno, NV.
[5] J.L. Neuringer, J. Fluid. Mech. 7 (1960) 287–301.
[6] D.T. Swift-Hook, J.K. Wright, J. Fluid. Mech. 15 (1962) 97–110.
[7] C. Carter, Brit. J. Appl. Phys. 17 (1966) 863–871.
[8] I. Inoue, M. Ishikawa, J. Umoto, Energy Conversion and Management 33 (1992) 873–884.
[9] Y. Inui, H. Ito, T. Ishida, Energy Conversion and Management 45 (2004) 1993–2004.
[10] B. Sahin, A. Kodal, H. Yavuz, J. Phys. D: Appl. Phys. (1996) 1473–1475.
[11] B. Sahin, A. Kodal, A.S. Otkem, J. Phys. D: Appl. Phys. (1999) 1832–1841.
[12] T. Matsuo, M. Ishikawa, J. Umoto, Energy Conversion and Management 39 (1998) 915–925.
[13] B.S. Bhadoria, A. Chandra, Energy Conversion and Management 40 (1999) 1985–1995.
[14] L. Chen, J. Gong, F. Sun, C. Wu, Energy Conversion and Management 43 (2002) 2085–2095.
[15] G. Ibáñez, S. Cuevas, Mariano López de Haro, Energy Conversion and Management 43 (2002) 1757–1771.
[16] V.S. Bajovi, Energy Conversion and Management 37 (1996) 1753–1764.
[17] G.N. Vanderplaats, ADS—a Fortran program for automated design synthesis, version 1.10, NASA CR-177985, September, 1985.
[18] S.O. Macheret, M.N. Shneider, R.B. Miles, External supersonic flow and scramjet inlet control by MHD with electron beam ionizer, in: AIAA-2001-0492, 39th AIAA Aerospace Sciences Meeting and Exhibit, 8–11 January 2001, Reno, NV.
[19] P. Palm, E. Ploenjes, I.V. Adamovich, J.W. Rich, E-beam sustained low-power budget air plasmas, in: AIAA 2002-0637, 40th AIAA Aerospace Sciences Meeting & Exhibit, 14–17 January 2002, Reno, NV.
[20] A.L. Kuranov, E.G. Sheikin, MHD control on hypersonic aircraft under "AJAX" concept. Possibilities of MHD generator, in: 40th AIAA Aerospace Sciences Meeting, January 2002 Reno, NV.
[21] R.J. Rosa, Magnetohydrodynamic Energy Conversion, McGraw Hill Book Company, 1968.